

Supporting Information

Exploring the Computational Design of Anionic Spin-Crossover Systems

Laia Navarro^[1] and Jordi Cirera^{[1]}*

[1] Departament de Química Inorgànica i Orgànica and Institut de Recerca de Química Teòrica i Computacional, Universitat de Barcelona, Diagonal 645, 08028 Barcelona, Spain

e-mail: jordi.cirera@qi.ub.es

DFT Benchmark for the $[\text{Fe}(\text{OEt-L}_1\text{-pH})(\text{NCS})_3]^-$ system	S1
Experimental values for different $[\text{Fe}(\text{R}_1\text{-L}_1\text{-pR}_2)(\text{L}_2)_3]^-$ reported systems	S2
Schematic d-based Molecular Orbital Diagrams for the $[\text{Fe}(\text{OEt-L}_1\text{-pH})(\text{L}_2)_3]^-$ systems ($\text{L}_2 = \text{NCO}^-$, NCS^- , NCSe^- and NCBH_3^-)	S3
Computed $T_{1/2}$ vs. the σ_p Hammett parameters for the $[\text{Fe}(\text{OEt-L}_1\text{-pR}_2)(\text{L}_2)_3]^-$ systems	S4
Computed ΔE and $T_{1/2}$ for the $[\text{Fe}(\text{OEt-L}_1\text{-pR}_2)(\text{NCO})_3]^-$ systems	S5
Cartesian coordinates and output calculations additional data	S6
Counterion effect control calculations	S7

S1. DFT Benchmark for the $[\text{Fe}(\text{OEt-L}_1\text{-pH})(\text{NCS})_3]^-$ system

<i>Method</i>	ΔE	ΔH	ΔS	$T_{1/2}$
TPSSh	6.94	5.59	24.67	226
OPBE	2.39	0.79	22.29	35
OLYP	-9.39	-10.89	21.44	-508
B3LYP	-7.83	-9.14	23.78	-384
B3LYP*	-5.54	-6.86	21.65	-317
M06L	-4.84	-6.30	19.77	-319

Table 1: Computed ΔE , ΔH , ΔS and $T_{1/2}$ for the $[\text{Fe}(\text{OEt-L}_1\text{-pH})(\text{NCS})_3]^-$ systems.

Electronic Energies and Enthalpies in $\text{kcal}\cdot\text{mol}^{-1}$. Entropies in $\text{cal}\cdot\text{K}^{-1}\cdot\text{mol}^{-1}$ and all temperatures in K. Experimental value for $T_{1/2} = 132$ K

S2. Experimental values for different $[\text{Fe}(\text{R}_1\text{-L}_1\text{-pR}_2)(\text{L}_2)_3]^-$ reported systems.

<i>System</i>	<i>Counterion</i>	<i>T</i> _{1/2}	<i>Refcode</i>	<i>reference</i>
$[\text{Fe}(\text{OEt-L}_1\text{-pH})(\text{NCS})_3]^-$	$[\text{NEt}_4]^+$	135	IROMOU	1
$[\text{Fe}(\text{OEt-L}_1\text{-pH})(\text{NCS})_3]^-$	$[\text{Fe}(\text{py}_3\text{C-OEt})_2]^+$	205	ZANLEJ	2
$[\text{Fe}(\text{OEt-L}_1\text{-pH})(\text{NCBH}_3)_3]^-$	$[\text{Fe}(\text{py}_3\text{C-OEt})_2]^+$	245(1), 380(2)	ZANLOT ^[a]	2
$[\text{Fe}(\text{OH-L}_1\text{-pH})(\text{NCS})_3]^-$	$[\text{NEt}_4]^+$	224(T [↑]) 246(T [↓])	XOPDAJ	3
$[\text{Fe}(\text{CH}_3\text{-L}_1\text{-pH})(\text{NCS})_3]^-$	$[\text{NBu}_4]^+$	330	IHEKEN	4
$[\text{Fe}(\text{CH}_3\text{-L}_1\text{-pH})(\text{NCS})_3]^-$	$[\text{PPh}_4]^+$	290	UXOHEW	5
$[\text{Fe}(\text{CH}_3\text{-L}_1\text{-pH})(\text{NCS})_3]^-$	$[\text{NMe}_4]^+$	313.4	-	6
$[\text{Fe}(\text{Et-L}_1\text{-pH})(\text{NCS})_3]^-$	$[\text{NMe}_4]^+$	338.2	-	6
$[\text{Fe}(\text{nPr-L}_1\text{-pH})(\text{NCS})_3]^-$	$[\text{NMe}_4]^+$	298.4	VULHES	6
$[\text{Fe}(\text{nBu-L}_1\text{-pH})(\text{NCS})_3]^-$	$[\text{NMe}_4]^+$	315.4	KUYFES	6
$[\text{Fe}(\text{Py-L}_1\text{-pH})(\text{NCS})_3]^-$	$[\text{Fe}(\text{py}_4\text{C})_2]^+$	161	GECHED	7
$[\text{Fe}(\text{nR-L}_1\text{-pH})(\text{NCS})_3]^-$	$[\text{NMe}_4]^+$	185.6	RIDGUJ	8

[a] = two-step transition

py₃C-OEt = tris(2-pyridyl)ethoxymethane

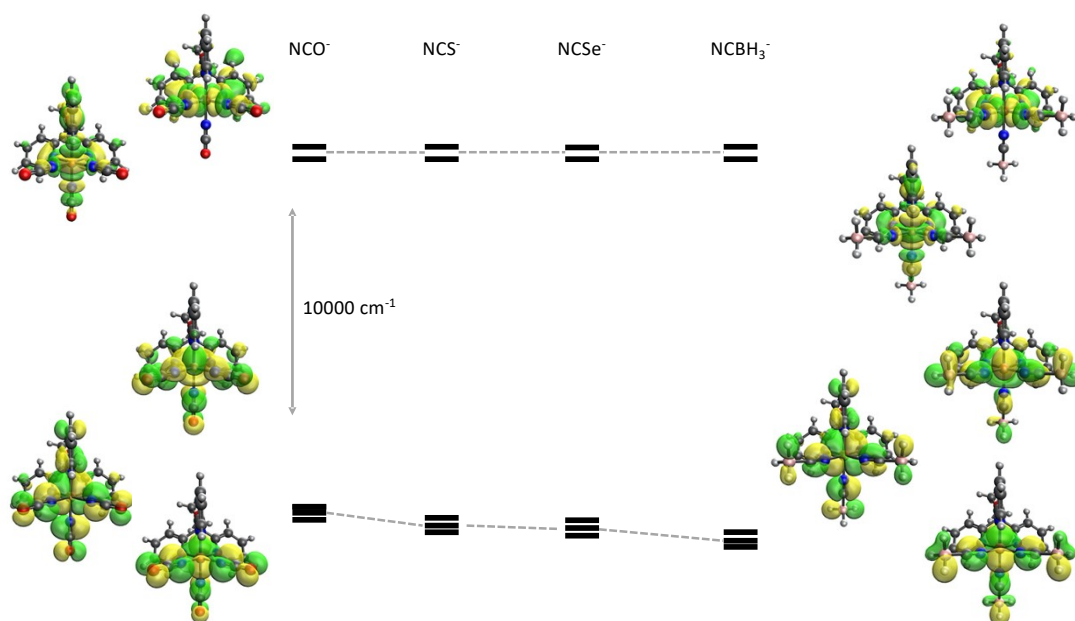
py₄C = tetrakis(2-pyridyl)methane

nR = nonadecane

References:

- 1 E. Cuza, C. D. Mekuimemba, N. Cosquer, F. Conan, S. Pillet, G. Chastanet and S. Triki, *Inorg. Chem.*, 2021, **60**, 6536–6549.
- 2 E. Cuza, S. Benmansour, N. Cosquer, F. Conan, S. Pillet, C. J. Gómez-García and S. Triki, *Magnetochemistry*, 2020, **6**, 26.
- 3 M. Yamasaki and T. Ishida, *Polyhedron*, 2015, **85**, 795–799.
- 4 M. Yamasaki and T. Ishida, *J. Mater. Chem. C*, 2015, **3**, 7784–7787.
- 5 T. Ishida, T. Kanetomo and M. Yamasaki, *Acta Crystallogr. Sect. C Struct. Chem.*, 2016, **72**, 797–801.
- 6 A. Kashiro, W. Kohno and T. Ishida, *Inorg. Chem.*, 2020, **59**, 10163–10171.
- 7 N. Hirose, Y. Oso and T. Ishida, *Chem. Lett.*, 2012, **41**, 716–718.
- 8 A. Kashiro, K. Some, Y. Kobayashi and T. Ishida, *Inorg. Chem.*, 2019, **58**, 7672–7676.

S3. Schematic d-based Molecular Orbital Diagrams for the $[\text{Fe}(\text{OEt-L}_1\text{-pH})(\text{L}_2)_3]^-$ systems ($\text{L}_2 = \text{NCO}^-$, NCS^- , NCSe^- and NCBH_3^-). Bottom table, energies (in cm^{-1}) of the five d-based MOs upon the AILFT interpretation of the NEVPT2 calculation on the S=0 optimized geometry.

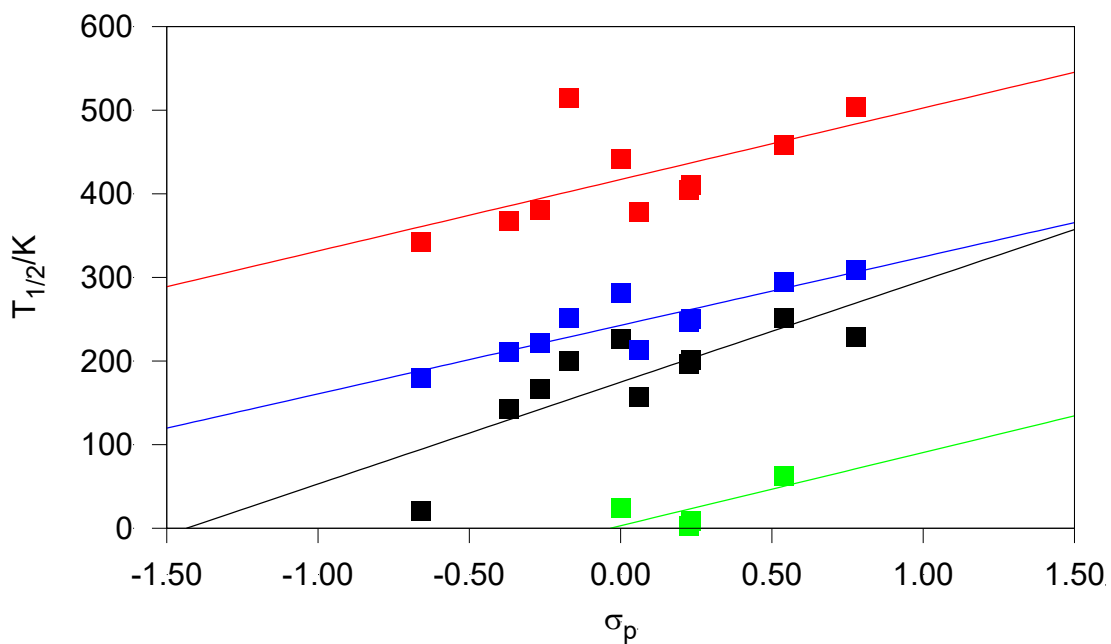


NCO^-	NCS^-	NCSe^-	NCBH_3^-
0	0	0	0
259.1	307.9	315.6	307
544.8	599.9	610.3	618
17199.5	17717.7	17827.2	18255.8
17858.2	18390.2	18513.9	18950.1

S4. Computed $T_{1/2}$ vs. the σ_p Hammett parameter for the $[\text{Fe}(\text{OEt-L}_1\text{-pR}_2)(\text{L}_2)_3]^-$ systems.

L_2 are in green (NCO^-), black (NCS^-), blue (NCSe^-) and red (NCBH_3^-), and

$\text{R}_2 = -\text{NH}_2, -\text{OH}, -\text{OMe}, -\text{Me}, -\text{F}, -\text{H}, -\text{Cl}, -\text{Br}, -\text{CF}_3$ and $-\text{NO}_2$.



The corresponding R^2 values are 0.75, 0.64, 0.76 and 0.40 respectively for NCO^- , NCS^- , NCSe^- and NCBH_3^- .

S5. Computed ΔE and $T_{1/2}$ for the $[\text{Fe}(\text{OEt-L}_1\text{-pR}_2)(\text{NCO})_3]^-$ systems. All energies in $\text{kcal}\cdot\text{mol}^{-1}$ and all temperatures in K.

$[\text{Fe}(\text{OEt-L}_1\text{-pR}_2)(\text{NCX})_3]^-$	NCO^-	
	ΔE	$T_{1/2}$
$\text{R}_2 = \text{OH}$	0.25	-38
$\text{R}_2 = \text{OMe}$	-5.07	-307
$\text{R}_2 = \text{Me}$	1.20	-2
$\text{R}_2 = \text{H}$	1.73	24
$\text{R}_2 = \text{Cl}$	1.33	3
$\text{R}_2 = \text{Br}$	1.48	9
$\text{R}_2 = \text{CF}_3$	2.64	62

S6. A data set collection of computational results is available in the ioChem-BD repository^[1] and can be accessed via <https://doi.org/10.19061/iochem-bd-6-152>

[1] Álvarez-Moreno, M.; de Graaf, C.; Lopez, N.; Maseras, F.; Poblet, J.M.; Bo, C. J. Chem. Inf. Model. 2015, 55, 95,103.

S7. Counterion effect control calculations

The effect of adding counterions to the studied systems was calibrated doing two sets of control calculations.

First, we studied if adding different counterions had a significant impact on the spin-state energy gaps. This was done by computing the $[\text{Fe}(\text{CH}_3\text{-L}_1\text{-pH})(\text{NCS})_3][\text{C}]^-$ where C could be $[\text{NMe}_4]^+$, $[\text{NEt}_4]^+$ or $[\text{PPh}_4]^+$. Results are summarized below:

System	Refcode	Counterion	ΔE	$\Delta E(\text{BSSE})$	ΔH	ΔS	$T_{1/2}$
$[\text{Fe}(\text{CH}_3\text{-L}_1\text{-pH})(\text{NCS})_3]^-$		-	10.48	10.48	9.15	23.50	389
$[\text{Fe}(\text{CH}_3\text{-L}_1\text{-pH})(\text{NCS})_3]^-$	IHEKEN	$[\text{NBu}_4]^+$	12.55	11.71	11.29	21.075	536
$[\text{Fe}(\text{CH}_3\text{-L}_1\text{-pH})(\text{NCS})_3]^-$	UXOHEW	$[\text{PPh}_4]^+$	12.37	11.46	11.04	24.136	458
$[\text{Fe}(\text{CH}_3\text{-L}_1\text{-pH})(\text{NCS})_3]^-$	VULHES	$[\text{NMe}_4]^+$	12.83	12.63	11.49	21.361	538

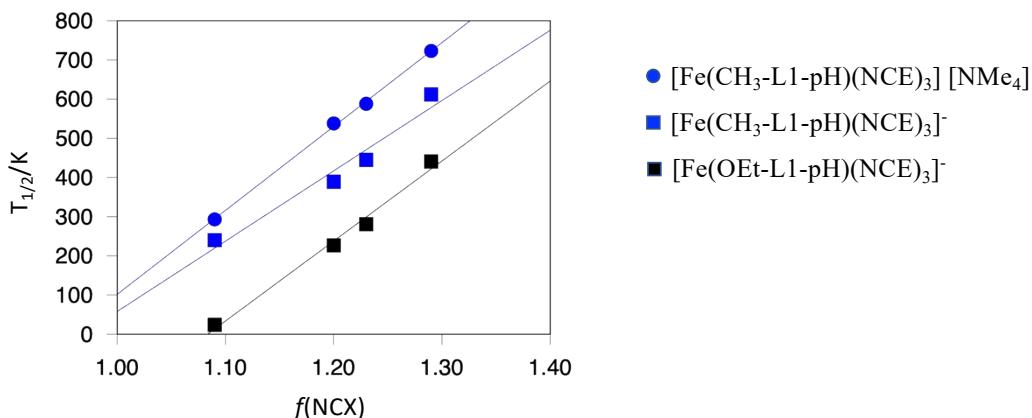
Computed spin-state energy gap (ΔE), enthalpy (ΔH), entropy (ΔS) and estimated $T_{1/2}$ for the $[\text{Fe}(\text{CH}_3\text{-L}_1\text{-pH})(\text{NCS})_3]^-$ molecule, without and with different counterions. Energy and enthalpy in kcal/mol, entropy in cal·K⁻¹·mol⁻¹, and temperatures in K

As can be seen, once the spin-state energy gap is corrected for the basis set superposition error (BSSE), the spin-state energy gap changes very little, and the computed values are also quite close to the spin-state energy gap without counterion. Remarkably, the calculations can model the decrease in $T_{1/2}$ when the counterion is $[\text{PPh}_4]^+$, as observed experimentally (see table S2).

The second test was done by computing the whole series of $[\text{Fe}(\text{CH}_3\text{-L}_1\text{-pH})(\text{NCE})_3]^-$ (E = O, S, Se or BH₃) with and without counterions, and comparing this results with the ones computed for the $[\text{Fe}(\text{OEt-L}_1\text{-pH})(\text{NCE})_3]^-$ system. Results are provide in the table below.

NCE	f	$[\text{Fe}(\text{CH}_3\text{-L}_1\text{-pH})(\text{NCE})_3][\text{NMe}_4]$	$[\text{Fe}(\text{CH}_3\text{-L}_1\text{-pH})(\text{NCE})_3]^-$	$[\text{Fe}(\text{OEt-L}_1\text{-pH})(\text{NCE})_3]^-$
NCS ⁻	1.2	538	389	226
NCS ^{e-}	1.23	588	445	281
NCBH ₃ ⁻	1.29	723	612	441
NCO ⁻	1.09	293	240	24

f factors and computed transition temperatures for the $[\text{Fe}(\text{CH}_3\text{-L}_1\text{-pH})(\text{NCE})_3][\text{NMe}_4]$, $[\text{Fe}(\text{CH}_3\text{-L}_1\text{-pH})(\text{NCE})_3]^-$ and $[\text{Fe}(\text{OEt-L}_1\text{-pH})(\text{NCE})_3]^-$ (E = S, Se, O, BH₃) systems.



Correlation between the computed $T_{1/2}$ and the f factor for the $[\text{Fe}(\text{CH}_3\text{-L}_1\text{-pH})(\text{NCE})_3][\text{NMe}_4]$ (blue circle), $[\text{Fe}(\text{CH}_3\text{-L}_1\text{-pH})(\text{NCE})_3]^-$ (blue square) and $[\text{Fe}(\text{OEt-L}_1\text{-pH})(\text{NCE})_3]^-$ (black square) ($\text{E} = \text{O}, \text{S}, \text{Se}$ and BH_3).

As can be seen in the above figure, the effect of adding counterions does not alter the trends, and is inferior to the one produced by changing $\text{R}_1 = -\text{CH}_3$ to $\text{R}_1 = -\text{OEt}$.

From this results, one can see firstly that the reported trends do not change upon inclusion of the counterion. Secondly, the main driving effect is replacing the R_2 group from $-\text{OEt}$ to $-\text{CH}_3$, thus proving one more time that the electronically driven effects are properly captured by the reported methodology.